Food Microbiology 140 (2026) 105177

Contents lists available at ScienceDirect

Food Microbiology

journal homepage: www.elsevier.com/locate/fm

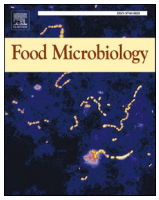

Ciprofloxacin resistance in *Salmonella* drives cross-protection to UV-C and HHP via *rpoD* mutation

Raúl Campillo [a], Ivo García-Penas [a], Dolores Rodrigo [b], Daniel Berdejo [a], Diego García-Gonzalo [a], Rafael Pagán [a,*]

[a] Departamento de Producción Animal y Ciencia de los Alimentos, Facultad de Veterinaria, Instituto Agroalimentario de Aragón-IA2 (Universidad de Zaragoza-CITA), Zaragoza, Spain
[b] Departamento de Conservación y Calidad, Instituto de Agroquímica y Tecnología de Alimentos IATA - Consejo Superior de Investigaciones Científicas (CSIC), Valencia, Spain

ARTICLE INFO

Keywords:
AMR
Genomic mutations
Pulsed electric fields
Ultraviolet irradiation
High hydrostatic pressure
Virulence

ABSTRACT

Antimicrobial resistance (AMR) remains a major public health concern, being the agri-food chain crucial in the emergence and dissemination of resistant pathogens such as *Salmonella* Typhimurium. Effective hygienization is key to prevent access of AMR bacteria into the agri-food chain. In this work, we investigated the consequences of ciprofloxacin (CIP) resistance acquisition in *S.* Typhimurium on tolerance to emerging non-thermal preservation technologies, including pulsed electric fields (PEF), ultraviolet C irradiation (UV-C) and high hydrostatic pressure (HHP). We focused on a CIP-resistant *S.* Typhimurium variant (SeT_{RV1}) previously shown to exhibit cross-protection to thermal treatments. While no significant differences were observed following PEF treatments, UV-C and HHP susceptibility was significantly reduced, resulting in survival increases ranging from approximately 32- to 2000-fold. We confirmed that a mutation in *rpoD* was the primary contributor to these phenotypes and associated with transcriptional changes in selected stress- and AMR-related genes, as determined by RT-qPCR. Virulence assessment using *Galleria mellonella* larvae revealed compensatory and divergent phenotypes associated with different mutations, ranging from reduced to enhanced virulence. Additional CIP-resistant variants harboring distinct mutations were subsequently evaluated, revealing that although PEF tolerance remained unaffected, several variants exhibited decreased susceptibility to UV-C, potentially linked to optimized DNA topology and enhanced oxidative stress responses. Overall, this study identifies *rpoD* as key driver of cross-protection to UV-C and HHP and highlights mutation-specific roles of *ramR* and *cyaA* in modulating UV-C tolerance and virulence, as well as *gyrA/gyrB* in increasing UV-C tolerance, with implications for food safety risk assessment in minimally processed foods.

1. Introduction

The slow progress in controlling antimicrobial resistance (AMR) in Europe demands urgent public health intervention (European Centre for Disease Prevention and Control, 2025). The magnitude of this challenge is reflected in the association of AMR bacteria with more than 35,000 deaths annually across Europe (European Centre for Disease Prevention and Control, 2022).

Within this context, cross-resistance in non-typhoidal *Salmonella* strains has become a particular focus of attention of food safety and public health authorities. In this setting, *cross-resistance* may be defined as the reduced susceptibility to multiple antibiotics, specifically to at least one antibiotic from three or more distinct families (Dawan and Ahn, 2020). In this regard, the agri-food chain has been identified as one of the key pathways for the emergence and dissemination of AMR foodborne pathogens (Lautan et al., 2025; Samtiya et al., 2022).

As an aggravating factor, cross-resistance can occur not only among antibiotics but also between compounds belonging to distant chemical families or even to physical stressors, such as the ones used in the agri-food chain (i.e., cross-protection). As a consequence, pathogens may acquire cross-protection against antibiotics through diverse mechanisms (Giacometti et al., 2021; Li et al., 2025; Liao et al., 2020). In this

* Corresponding author. Departamento de Producción Animal y Ciencia de los Alimentos, Facultad de Veterinaria, Instituto Agroalimentario de Aragón-IA2 (Universidad de Zaragoza-CITA), C/ Miguel Servet 177, 50013, Zaragoza, Spain.
E-mail address: pagan@unizar.es (R. Pagán).

https://doi.org/10.1016/j.fm.2026.105177
Received 5 April 2026; Received in revised form 11 May 2026; Accepted 26 May 2026
Available online 29 May 2026

manuscript, the term *cross-protection* is used as an umbrella concept to describe reduced susceptibility whereby adaptation or resistance to a given stressor (including antibiotics) results in a decreased susceptibility to other antibiotics and also to non-antibiotic stressors, including food processing and emerging non-thermal technologies. One well-recognized example is the cross-protection observed between antibiotics and biocides in biocide-resistant bacteria (Coombs et al., 2023; Milani et al., 2021). Similar phenomena have increasingly been reported in bacteria with acquired protection against food industry-related stressors, including food preservation methods (Álvarez-Molina et al., 2020; Berdejo et al., 2022; Gayán et al., 2017; Guillén et al., 2025; Milani et al., 2021; Pagán et al., 2024).

Notably, such cross-protection has most often been described as a collateral effect of adaptation to non-antibiotic stressors, rather than as a consequence of AMR itself. Almost 40 years ago, a spontaneous mutation in *ubiF* conferring bleomycin resistance in an *Escherichia coli* strain was suggested to induce cross-protection against heat treatments as a pleiotropic effect (Collis and Grigg, 1989). A similar phenotype was later reported by Søballe and Poole (2000). Since then, the contribution of AMR to cross-protection against thermal treatments has been investigated repeatedly, often yielding negative or inconclusive results (Hong et al., 2023; Park et al., 2021; Walsh et al., 2001, 2005). This is largely because phenotypic outcomes were not directly compared with those of the actual susceptible parental strain, or because cross-protection was simply not considered (Oniciuc et al., 2019).

Building on this background, we recently evolved *S.* Typhimurium toward ciprofloxacin (CIP) resistance using adaptive laboratory evolution (ALE) experiments and demonstrated a positive association between induced mutations conferring CIP resistance and remarkable cross-protection against thermal treatments (Campillo et al., 2025). This association was validated through a gene replacement procedure (Campillo et al., 2026) in which the mutated alleles, individually and in combination, were relocated into the genome of the parental strain (SeT), generating the isogenic mutants (SeT_{rpoD}, SeT_{cyaA}, SeT_{ramR}, $SeT_{rpoD/cyaA}$, $SeT_{rpoD/ramR}$ and $SeT_{cyaA/ramR}$). This is why, given that the underlying cross-protection mechanisms appear to be broad-spectrum and non-specific, we now aim to assess whether similar effects extend to alternative physical inactivation technologies, particularly emerging non-thermal approaches. To our knowledge, experimental evidence linking AMR to altered tolerance against emerging non-thermal food preservation technologies is limited. Moreover, since AMR and virulence are not two independent traits and can be negatively or positively correlated (Cepas and Soto, 2020), cross-protection phenomena can be particularly relevant. If bacterial adaptation does not compromise virulence, the probability of getting foodborne infections increases, while simultaneously facilitating the dissemination of AMR from the food chain to consumers and limiting the effectiveness of antibiotic treatment during eventual infection. Investigating the genetic basis underlying these cross-protection phenomena is expected to provide key insights into virulence and microbial resistance mechanisms involved in response to emerging technologies. Therefore, we hypothesized that mutations conferring CIP resistance and thermal cross-protection could also influence bacterial susceptibility to non-thermal inactivation technologies, such as pulsed electric fields (PEF), ultraviolet C irradiation (UV-C), and high hydrostatic pressure (HHP), and virulence potential, although the outcome might depend on the specific cellular targets of each technology. Among emerging non-thermal technologies, PEF, UV-C, and high HHP represent three widely investigated approaches with distinct mechanisms of microbial inactivation: PEF primarily targets the cytoplasmic membrane through electroporation (Mañas and Pagán, 2005; Raso et al., 2016), UV-C mainly causes DNA damage through photochemical reactions and oxidative stress that impair cellular repair mechanisms (Song et al., 2019), and HHP induces broader cellular damage including membrane perturbation and protein denaturation (Sehrawat et al., 2021). Therefore, this study aimed to determine whether the acquisition of CIP resistance in *S.* Typhimurium modulates bacterial tolerance to these non-thermal technologies. Specifically, we firstly evaluated the response of a CIP-resistant variant (SeT_{RV1}) to PEF, UV-C and HHP, including validation in liquid food matrices for HHP. Secondly, we investigated the contribution of the mutations present in SeT_{RV1} using its derived isogenic mutants (SeT_{rpoD}, SeT_{cyaA}, SeT_{ramR}, $SeT_{rpoD/cyaA}$, $SeT_{rpoD/ramR}$ and $SeT_{cyaA/ramR}$). Afterwards, we examined the basal transcriptional levels of selected stress-related genes prior to inactivation treatments. The consequences of these mutations for virulence were also assessed, and we explored whether additional CIP-resistant variants (SeT_{RV2}-SeT_{RV5}) display altered tolerance to PEF and UV-C.

2. Materials and methods

2.1. Bacterial strains

The strains used in this study were *Salmonella enterica* subsp. *enterica* serovar Typhimurium strain LT2 (SeT) from the Spanish Type Culture Collection (CECT 722), and five ciprofloxacin-resistant variants (SeT_{RV1}-SeT_{RV5}), previously isolated through ALE experiments under CIP pressure following whole-genome sequencing (Campillo et al., 2025). Whole-genome sequencing of SeT_{RV1} revealed three induced mutations: a single-nucleotide variation in *ramR* (G74C), a three-nucleotide insertion in *rpoD* (GCC 1764), resulting in an additional alanine residue, and a frameshifting deletion in *cyaA* (ATGA 2252) (Campillo et al., 2025). This study also includes strains individually (SeT_{rpoD}, SeT_{cyaA} and SeT_{ramR}) and in combination ($SeT_{rpoD/cyaA}$, $SeT_{rpoD/ramR}$ and $SeT_{cyaA/ramR}$) carrying the mutated alleles, which were constructed following a gene replacement approach as described elsewhere (Campillo et al., 2026). This strategy provided a clearer picture to attribute the phenotypic changes observed in SeT_{RV1} to specific genotypic alterations. Throughout this study, all strains were stored at −80 °C in cryovials containing glycerol (20% *v/v*).

2.2. Growth conditions

Plates of tryptone soya agar (Oxoid, Basingstoke, United Kingdom) supplemented with 0.6% (*w/v*) yeast extract (Oxoid; TSAYE) were prepared from the cryovials on a weekly basis. To prepare the working bacterial cultures, test tubes containing 5 mL of cation-adjusted Mueller Hinton broth (Sigma-Aldrich, Saint Louis, USA; MHB) were inoculated with a single colony and incubated at 37 °C overnight (Incubig, Selecta, Barcelona, Spain) under aerobic conditions in an orbital shaker (130 rpm; Vibramax 100, Heidolph, Schwaback, Germany). These overnight subcultures were then used to inoculate flasks containing 10 mL of fresh MHB, reaching an initial concentration of 10^6 colony forming units per mL (CFU/mL), and incubated at 37 °C and 130 rpm for 24 h until stationary growth phase (~3×10^9 CFU/mL). Bacterial concentrations were verified via serial dilution in phosphate-buffered saline (Sigma-Aldrich; PBS) followed by spread-plating on TSAYE.

2.3. Assessment of bacterial tolerance against non-thermal technologies

Before treatments, cells from stationary phase cultures were harvested via centrifugation (10,000×*g* for 3 min) in a microcentrifuge (MiniSpin, Eppendorf, Hamburg, Germany) and resuspended in the treatment medium. Thereafter, the resuspended cells (~3×10^9 CFU/mL) were subjected to decimal dilutions in PBS to obtain a starting concentration of ~3×10^7 CFU/mL in the working suspensions, thereby initiating the treatments with emerging technologies. Treated samples were diluted in PBS, spread-plated on TSAYE, and incubated at 37 °C for 24 h. Microbial counts were taken in an automatic plate counter via image analysis (Analytical Measuring Systems, Protos, Cambridge, United Kingdom) in order to plot the $\log_{10}$ reduction ($\log_{10}[N_0/N_t]$) after each treatment condition. N_0 represents the CFU/mL at the beginning of the experiment, and N_t after t minutes of treatment. Survival risk was

estimated from differences in $\log_{10}$ reductions, in which each $\log_{10}$ unit corresponds to a 10-fold change in the survival fraction.

Three non-thermal emerging technologies for microbial inactivation in the food industry were selected: pulsed electric fields (PEF), ultraviolet C irradiation (UV-C), and high hydrostatic pressure (HHP). PEF and UV-C treatments were conducted in McIlvaine buffer to minimise temperature increases and turbidity-related interferences, respectively, whereas HHP was additionally evaluated in liquid food matrices. Treatment times and intensities were selected based on preliminary experiments to achieve substantial but non-complete inactivation, allowing comparison of strain-dependent responses.

2.3.1. Pulsed electric fields (PEF)

PEF treatments were conducted using a dedicated PEF system (Vitave, Prague, Czech Republic) which provided monopolar square-wave pulses. The batch treatment chamber consisted of a cylindrical sterile plastic tube mounted between two stainless-steel electrodes, with an interelectrode distance of 0.25 cm and an electrode area of 2.01 cm^2. The treatment medium of the working inoculum (3×10^7 CFU/mL) was citrate-phosphate McIlvaine buffer adjusted to pH 7.0 and 1 mS/cm of conductivity, elaborated from citric acid monohydrate (PanReac, Darmstadt, Germany) and disodium hydrogen phosphate (PanReac). The necessary volume to fill the treatment chamber (~500 μL) was then transferred and subjected to 50 pulses of 1 μs at 1 Hz to bacterial suspensions at a field intensity of 30 kV/cm, implying a specific energy of around 45 kJ/kg. The total specific energy was estimated from the energy delivered per pulse, calculated using the applied voltage (7.5 kV), pulse width (1 μs), equivalent resistance (124.3 Ω), sample density (~1,000 kg/m^3) and treatment volume (0.5 mL). Under these conditions, the specific energy was approximately 0.9 kJ/kg per pulse. Pulses were monitored using a high-voltage probe (P6015A, Tektronik, Wilsonville, OR, USA) connected to an oscilloscope (TDS 220, Tektronik). The temperature of bacterial suspensions was checked after treatments using a K-type thermocouple probe connected to a data collection system (Almemo 2450, Ahlborn, Holzkirchen, Germany), never exceeding 35 °C in mock tests.

2.3.2. Ultraviolet C irradiation (UV-C)

UV-C treatments were carried out using a 32 W UV-C lamp (VL-208G, Vilber, Germany) mounted on the upper interior of a ventilated cabinet. Microtiter plates containing the bacterial suspensions were placed beneath the lamp under static conditions. Each plate was sealed with two layers of gas-permeable film (BREATHseal, Greiner Bio-One, Frickenhausen, Germany). Treatments were performed in McIlvaine buffer (pH 7.0), with a final volume of 200 μL of working inoculum per well. Samples were exposed to an irradiance of 0.50 ± 0.02 mW/cm^2 for 30 s, corresponding to an approximate fluence (UV-C dose) of 15 mJ/cm^2. Irradiance was measured with a UVX radiometer (UVP, LLC, Upland, CA, USA), and temperature never exceeded 35 °C.

2.3.3. High hydrostatic pressure (HHP)

HHP treatments were performed as previously described by Diez-Sánchez et al. (2020). Briefly, a pilot-scale unit (High-Pressure Food Processor, EPSI NV, Temse, Belgium) with a 2.35 L vessel filled with a water-ethylene glycol as a pressurizing medium was used. For each treatment, 1.5 mL polystyrene tubes were completely filled with the working inoculum, leaving no headspace, and sealed with two layers of Parafilm to prevent leakage or filtration. In this case, two liquid food matrices with contrasting physicochemical properties were used as treatment media to validate the results obtained in laboratory media under food-relevant conditions: commercial skimmed milk (Central Lechera Asturiana, Siero, Spain; pH 6.67 measured at 23.8 °C), and orange juice (Don Simón, Madrid, Spain; pH 3.63 measured at 23.8 °C). Prior to pressurization, all tubes were placed in polyethylene bags and thermosealed (Multivac, Hünenberg, Switzerland). Samples were pressurized at 350 MPa (for 5 min in orange juice and for 20 min in skimmed milk) using a compression rate of 300 MPa/min and a decompression time of less than 1 min. These conditions were selected to achieve at least a 3-$\log_{10}$ reduction of SeT based on preliminary experiments (data not shown), allowing meaningful comparison of inactivation responses between strains. Pressure, time, and temperature were automatically controlled, never exceeding 35 °C. Following treatment, samples were immediately removed from the vessel and kept on ice for the shortest possible time before diluting to obtain microbial counts.

2.4. Gene expression analysis

Gene expression levels were quantified by RT-qPCR in SeT_{rpoD} and SeT immediately before the inactivation treatments to evaluate a potential stress-prepared transcriptional state associated with the hypothesized attenuation of RpoD activity. Our approach involved reverse transcription of RNA followed by real-time quantification, which provides a sensitive and reliable method to assess gene expression (Aviv and Gal-Mor, 2018).

2.4.1. Total RNA isolation and cDNA synthesis

Total RNA was extracted from two biological replicates of both SeT and SeT_{rpoD}. Each sample was centrifuged and resuspended in the treatment media as described previously (Section 2.3.). Bacteria were enzymatically lysed, digested, and RNA was stabilized using the RNAprotect Bacteria Reagent (Qiagen, Hilden, Germany). Total RNA was then isolated with the RNeasy Mini Kit (Qiagen) following the manufacturer's instructions. Residual genomic DNA was removed using the RNase-Free DNase set (Thermo Fisher Scientific, Waltham, MA, USA). RNA integrity was assessed using Qubit 4 Fluorometer and Qubit RNA IQ Assay (Thermo Fisher Scientific), yielding integrity values above nine, considered undegraded. Total RNA concentration and purity was measured with a microvolume spectrophotometer (DS-11 FX, DeNovix, Wilmington, DE, USA), with $OD_{260/280}$ ratios between 2.0 and 2.2. All RNA samples were stored at −80 °C until further use.

We synthesized the first-strand complementary DNA (cDNA) using the Superscript First-Strand Synthesis System for RT-PCR (Invitrogen, Camarillo, CA, USA) with random hexamer primers in a regular thermocycler (T100 Thermal Cycler, Bio-rad, Hercules, CA, USA).

2.4.2. Reverse transcription-quantitative polymerase chain reaction (RT-qPCR)

RT-qPCR assays were performed using a CFX Deepwell Real-Time PCR System (Bio-rad) with SYBR Green Master Mix (Bio-rad). The amplification protocol consisted of an initial enzyme activation step at 95 °C for 3 min, followed by 40 cycles of denaturation at 95 °C for 15 s and combined annealing and extension at 60 °C for 1 min, during which fluorescence was measured. Melting curve analysis was carried out from 60 to 95 °C, with temperature increments of 0.5 °C every 5 s. Specificity of amplification was confirmed by melting curve analysis, showing a single peak for each primer pair.

Gene expression was quantified using an absolute quantification approach based on standard curves. *Ct* (cycle threshold) values were converted to gene copy numbers, and subsequently used in the linear regression equations (see Supplementary materials) derived from the standard curves to estimate gene template concentrations (Yun et al., 2006). These values were then normalized to the 16S rRNA reference gene to account for differences in template quantity (Brankatschk et al., 2012; Livak and Schmittgen, 2001).

The primers used targeted key genes involved in bacterial stress responses and transcriptional regulation (Table 1). These included alternative sigma factors that coordinate diverse stress-adaptation pathways (*rpoD, rpoE, rpoH, rpoN,* and *rpoS*), as well as genes involved in stress defense and cellular protection mechanisms, such as protein quality control (*dnaK, htrA*), oxidative stress response (*soxR*), and global stress regulation through the stringent response (*spoT*). These genes were selected since they represent major regulatory and protective pathways

Table 1
List of primers used for RT-qPCR analysis of *Salmonella enterica* subsp. *enterica* serovar Typhimurium str. LT2 parental strain (SeT) and its isogenic mutant with the mutated *rpoD* allele (SeT_{rpoD}). 16S rRNA was used as control for normalization.

Gene	Primer sequence (5' → 3')	Amplicon length (bp)	Amplicon Tm (°C)	Regression coefficient (R^2)
rpoD	Fw: AAC CTG GTT CAA TGC CGC TA Rv: ACA TGC GAC GGT TGA TGT CT	158	86.0-86.5	0.999
rpoS	Fw: ACA CCA CGC AAG ATG ACG AT Rv: GAC CGA TTT CAC GGC CTA CA	147	86.0	0.999
rpoH	Fw: TAG CTT TAG CCC CTG TTG GC Rv: CAA CAA AGC GCA GGT GAG AC	162	87.5-88.0	0.991
rpoE	Fw: ACG TTC CCG ATG TCG TAC AG Rv: AAC CAG GTA GTT CTT CGC GG	128	82.5	0.998
rpoN	Fw: GCT GGT ACG CAA GCA TAA CG Rv: TCG TTA CGG CTT TCA AGG CT	186	86.0	0.995
dnaK	Fw: TCG ACG AAG TTG ATG GCG AA Rv: TTG GCT TTT TCT GCG GCT TC	190	86.0	0.997
htrA	Fw: GCA GCC AGA GTC AGG TTG AT Rv: TAC GCA GCT CGG CGA TAT TT	198	87.0	0.998
soxR	Fw: CGT TAA GCG CGA AAG AGT GG Rv: GGA CAG TCG CTA CGC GAT AA	139	87.0-87.5	0.995
spoT	Fw: TGC AGG ATA TCC GCG TCA TC Rv: AAT ACC TAA ACG GTG CGC CA	146	86.5-87.0	0.999
16S	Fw: CAG AAG AAG CAC CGG CTA ACT C Rv: GCG CTT TAC GCC CAG TAA TT	87	85.0-85.5	0.998

Fw: forward; Rv: reverse; bp: base pairs; Tm: melting temperature

known to mediate bacterial adaptation to environmental and antimicrobial stresses. The "Primer designing tool" developed by the U.S. National Center for Biotechnology Information (NCBI) was used to design and select the primers used.

2.5. In-vivo virulence using Galleria mellonella infection

The injection of pathogenic microorganisms into *G. mellonella* larvae is a widely used model for evaluating microbial virulence due to its reliability, operational simplicity, the absence of complex ethical considerations, and the presence of an immune response similar to that of mammals (Ménard et al., 2021; Tsai et al., 2016).

Larvae of the wax moth *G. mellonella* (Reptilmadrid S.L., Madrid, Spain) were stored in wood shavings, in the dark, at room temperature and used within 3 days from shipment. To avoid sampling biases, larvae were preliminary inspected to randomly select healthy individuals with no visible melaninization or deformities. To prepare the bacterial injection suspensions, several isolated colonies were generously swabbed using a sterile cotton swab and transferred into 15 mL sterile tubes containing 5 mL of PBS. The resulting suspensions were centrifuged at 3,000×*g* for 15 min (Megafuge 1.0R, Heraeus, Hanau, Germany), and the supernatant was discarded. Bacterial pellets were resuspended in 1 mL of sterile PBS. After washing, the concentration of each bacterial suspension was standardized by adjusting the optical density at 600 nm (OD_{600}) using semi-micro polystyrene cuvettes in a spectrophotometer (Libra S12, Biochrom Ltd, Cambridge, United Kingdom) to 0.5 McFarland (OD_{600} = 0.65-0.75), corresponding to ~10^8 CFU/mL (Farzana et al., 2018). Once standardized, serial decimal dilutions were performed with PBS to obtain the final concentrations used to inject 10 μL. Based on prior tests (data not shown), each bacterial strain was injected at two microbial concentration levels: 10^4 and 10^5 CFU/mL approximately, using sterile 1 mL syringes with 25-gauge needles (B. Braun, Melsungen, Germany). Injections were conducted through the rear left proleg (Kay et al., 2019; Yang et al., 2017), at an angle of 10-20° to secure direct access to the hemocoel without damaging vital organs. Larvae were kept in refrigeration for 30 min to reduce their activity prior to injections.

Following injection, the larvae were incubated at 37 °C for 24, 48, and 72 h, and the number of live and dead larvae was recorded at each time point. Larvae can survive at this incubation temperature, making it suitable for studying temperature-dependent microbial virulence factors (Tsai et al., 2016). Survival was expressed as percentage survival based on the number of live larvae per replicate. Each condition was performed in triplicate, with ten larvae per replicate. A control group was also included, injected with 10 μL of sterile PBS. Larvae were considered as dead when no movement was detected when gently prodded.

2.6. Statistical analysis

Statistical analysis and graph construction were performed using GraphPad Prism® program (GraphPad Software, San Diego, CA, USA). Results regarding lethal treatments were obtained from at least three independent experiments conducted with different bacterial cultures on different working days. Log_{10} reductions and survival percentages are displayed as the mean ± standard deviation of no less than 3 replicates. Normality of the data was evaluated using Kolmogorov-Smirnov and Shapiro-Wilk tests. Parametric data were analyzed using *t*-test or one-way ANOVA. When significant differences were detected, Tukey's post-hoc test was applied. Nonparametric data were analyzed using the Mann-Whitney *U* test or Kruskal-Wallis' test. Differences in normalized gene abundance between strains after RT-qPCR were assessed by comparing the normalized gene copy numbers, with technical replicates merged prior to analysis. Kaplan-Meier survival curves for *G. mellonella* infections were constructed to evaluate larval survival over time. In this case, statistical differences between survival curves were assessed using the Mantel-Cox (log-rank) test with multiple comparisons between strains. Results sharing at least one letter are not significantly different ($p > 0.05$), whereas different letters or asterisks (*) indicate significant differences ($p \leq 0.05$).

3. Results

Based on the hypotheses previously outlined, we first examined whether the ciprofloxacin-resistant variant SeT_{RV1} exhibited altered tolerance to emerging non-thermal inactivation technologies compared with the parental strain SeT.

3.1. Cross-protection patterns in ciprofloxacin-resistant variant SeT_{RV1} against emerging non-thermal technologies

The responses of SeT_{RV1} and the parental strain SeT were compared following treatments with three non-thermal inactivation technologies of distinct physical nature: PEF, UV-C, and HHP (Table 2).

Upon PEF treatments, no significant differences were observed between the inactivation of SeT_{RV1} and SeT ($p > 0.05$), suggesting that mutations do not affect PEF sensitivity under the conditions tested. In contrast, UV-C treatments revealed marked differences: while the SeT population was inactivated by 3.62 log_{10} cycles, only 1.03 log_{10} cycles of SeT_{RV1} were inactivated ($p \leq 0.05$), corresponding to a ~400-fold higher

Table 2
Comparative analysis of *Salmonella enterica* subsp. *enterica* serovar Typhimurium str. LT2 parental strain (SeT) and its ciprofloxacin-resistant variant (SeT_{RV1}) under different treatment conditions with emerging non-thermal inactivation technologies. Bacterial reduction is expressed as log_{10} reduction ± standard deviation. Relative survival risk increases are also indicated when significant. These conditions were selected to achieve at least a 3-log_{10} reduction of SeT.

Technology	Treatment conditions	Treatment medium	Strain	Log_{10} reduction (CFU/mL)	Survival risk increase
PEF	30 kV/cm, 50 pulses	McIlvaine pH 7.0	SeT	2.78 ± 0.32	Not significant ($p > 0.05$)
			SeT_{RV1}	3.34 ± 0.29	
UV-C	15 mJ/cm^2	McIlvaine pH 7.0	SeT	3.62 ± 0.41	~400-fold
			SeT_{RV1}	1.03 ± 0.26	
HHP	350 MPa 5 min	Orange juice	SeT	5.67 ± 0.10	~32-fold
			SeT_{RV1}	4.16 ± 0.27	
	350 MPa 20 min	Skimmed milk	SeT	3.78 ± 0.68	~2000-fold
			SeT_{RV1}	0.53 ± 0.46	

PEF: pulsed electric fields; UV-C: ultraviolet C irradiation; HHP: high hydrostatic pressure. Log_{10} reduction expressed as mean ± standard deviation. Fold-changes in survival risk were calculated from the difference in log_{10} reduction between strains. In all the treatments, N_0 ~3 × 10^7 CFU/mL.

survival risk. In the case of HHP, inactivation was also reduced in SeT_{RV1}. In orange juice, HHP treatment reduced SeT population by 5.67 log_{10} cycles, whereas SeT_{RV1} showed a smaller reduction of 4.16 log_{10} cycles ($p \leq 0.05$), corresponding to ~32-fold increase in survival risk. In skimmed milk, the difference was much more pronounced, with SeT reduced by 3.78 log_{10} cycles compared with only 0.53 log_{10} cycles for SeT_{RV1} ($p \leq 0.05$), corresponding to a ~2000-fold increase in survival risk.

3.2. Combined involvement of AMR-related mutations toward UV-C and HHP cross-protection in SeT_{RV1}

As previously reported, SeT_{RV1} harbors three induced mutations: a single-nucleotide variation in ramR (G74C), a three-nucleotide insertion in *rpoD* (GCC 1764), and a frameshifting deletion in *cyaA* (ATGA 2252) (Campillo et al., 2025). To determine the contribution of each mutation to the observed cross-protection phenotype after UV-C and HHP treatments, we analyzed a set of isogenic mutants carrying these alleles individually (SeT_{rpoD}, SeT_{cyaA}, and SeT_{ramR}) and in combination ($SeT_{rpoD/cyaA}$, $SeT_{rpoD/ramR}$, and $SeT_{cyaA/ramR}$) (Fig. 1).

All three mutations present in SeT_{RV1} contributed to varying degrees in cross-protection against UV-C. While mutations in *cyaA* and *ramR* contributed the least as observed in SeT_{cyaA} and SeT_{ramR} inactivation (2.43 and 2.69 log_{10} reduction, respectively; $p \leq 0.05$), mutated *rpoD* almost fully explained SeT_{RV1} cross-protection, since SeT_{rpoD} reached similar inactivation compared to SeT_{RV1} (1.24 log_{10} reduction; $p \leq 0.05$). When mutations were combined, no additive or synergistic effects were observed for *cyaA* when combined with *rpoD* or *ramR* mutations (1.09 and 2.51 log_{10} reduction for $SeT_{rpoD/cyaA}$ and $SeT_{cyaA/ramR}$, respectively). Interestingly, a slight antagonistic effect could be described when *rpoD* and *ramR* were present in the same genomic context: although no statistical differences were detected ($p > 0.05$), inactivation of $SeT_{rpoD/ramR}$ was 0.44 log_{10} cycles higher than SeT_{rpoD}.

As SeT_{RV1} also displayed cross-protection against HHP, we decided to further investigate the molecular bases of its reduced susceptibility, in a similar way to UV-C. In this case, HHP treatments were applied in orange juice (Fig. 2A) and skimmed milk (Fig. 2B), under conditions yielding approximately 4-6 log_{10} reduction of SeT, sufficient to characterize the observed cross-protection. Upon HHP treatments in orange juice, inactivation patterns similar to those observed for UV-C were detected. Single mutations in *cyaA* and *ramR* resulted in cross-sensitization, with inactivation levels exceeding the limit of detection. In contrast, mutation of *rpoD* significantly enhanced HHP tolerance, as

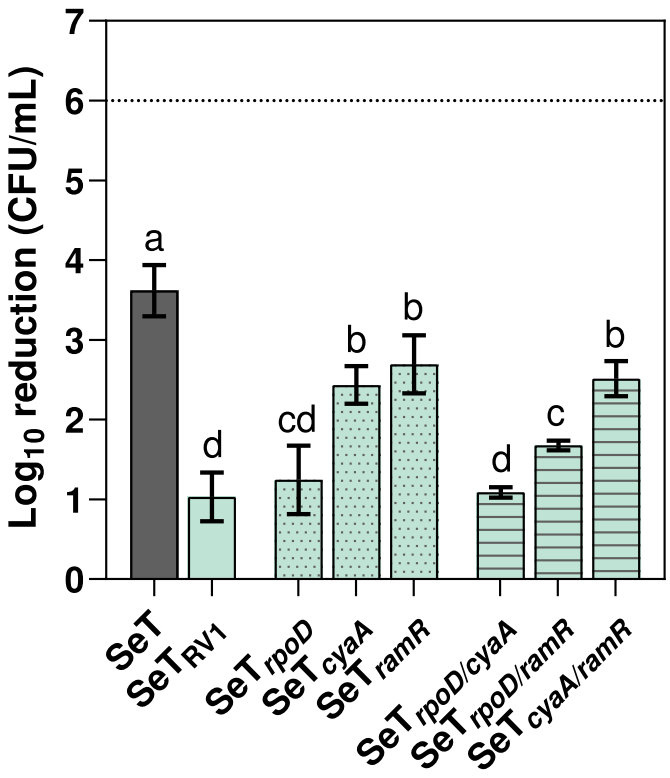

Fig. 1. Log_{10} reduction (log_{10} [N_0/N_t]) of *Salmonella enterica* subsp. *enterica* serovar Typhimurium str. LT2 parental strain (SeT), its ciprofloxacin-resistant variant (SeT_{RV1}), and the single- (SeT_{rpoD}, SeT_{cyaA}, SeT_{ramR}; bars filled with dots) and double-isogenic mutants ($SeT_{rpoD/cyaA}$, $SeT_{rpoD/ramR}$, $SeT_{cyaA/ramR}$; bars filled with horizontal lines) after performing lethal treatments with ultraviolet C irradiation (15 mJ/cm^2). Treatment medium was citrate-phosphate buffer at pH 7.0. Results expressed as means ± standard deviations (error bars). N_0 ~3 × 10^7 CFU/mL. Horizontal dotted line represents the detection limit. Different letters indicate significant differences ($p \leq 0.05$).

observed in both SeT_{RV1} (4.16 log_{10} reduction) and the single mutant SeT_{rpoD} (4.30 log_{10} reduction), compared with the parental strain SeT (5.67 log_{10} reduction; $p \leq 0.05$). As previously described, combining *rpoD* with the *ramR* allele exerted an antagonistic effect, reducing cross-protection conferred by the *rpoD* mutation. However, when *cyaA* and *ramR* mutations were combined, the cross-sensitization associated with the individual mutations was abolished (5.50 log_{10} reduction in $SeT_{cyaA/ramR}$), yielding inactivation levels comparable to those of SeT. This antagonistic interaction was further suppressed when all three mutations were in combination present in SeT_{RV1}, restoring the tolerant phenotype.

Similar trends were observed following HHP treatments in skimmed milk, although cross-protection was markedly enhanced compared with orange juice. In milk, SeT_{RV1} showed minimal inactivation (0.53 log_{10} reduction), whereas SeT exhibited substantially higher inactivation (3.78 log_{10} reduction). Again, the mutated *rpoD* allele emerged as the primary contributor to cross-protection, as SeT_{rpoD} showed similarly low inactivation levels (0.66 log_{10} reduction). In this case, both *cyaA* and *ramR* (SeT_{cyaA} and SeT_{ramR} inactivation levels surpassed limit of detection) exerted antagonistic effects on the protective contribution of *rpoD*, since $SeT_{rpoD/cyaA}$ and $SeT_{rpoD/ramR}$ were significantly more inactivated than SeT_{RV1} and SeT_{rpoD} (1.43 and 2.13 log_{10} reduction in $SeT_{rpoD/cyaA}$ and $SeT_{rpoD/ramR}$, respectively), yet still less inactivated than SeT.

3.3. Single mutation in rpoD increases basal expression of stress-responsive genes

To explore the potential regulatory effects associated with the *rpoD*

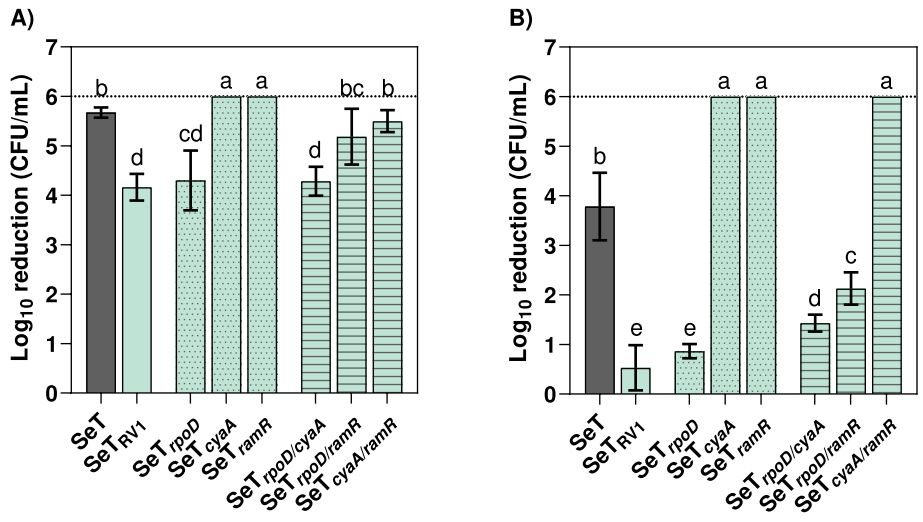

Fig. 2. Log_{10} reduction (log_{10} [N_0/N_t]) of *Salmonella enterica* subsp. *enterica* serovar Typhimurium str. LT2 parental strain (SeT), its ciprofloxacin-resistant variant (SeT_{RV1}), and the single- (SeT_{rpoD}, SeT_{cyaA}, SeT_{ramR}; bars filled with dots) and double-isogenic mutants ($SeT_{rpoD/cyaA}$, $SeT_{rpoD/ramR}$, $SeT_{cyaA/ramR}$; bars filled with horizontal lines) after performing lethal treatments with high hydrostatic pressure in **A)** orange juice (350 MPa for 5 min), and **B)** skimmed milk (350 MPa for 20 min). Results expressed as means ± standard deviations (error bars). N_0 ~3×10^7 CFU/mL. Horizontal dotted line represents the detection limit. Different letters indicate significant differences ($p \leq 0.05$).

mutation, we evaluated the basal expression of selected stress-responsive genes in the isogenic mutant SeT_{rpoD} compared with the parental strain SeT prior to the inactivation treatments.

Relative expression of alternative sigma factors that coordinate diverse stress-adaptation pathways (*rpoD, rpoE, rpoH, rpoN, rpoS*) and key genes involved in stress defense (*dnaK, htrA, soxR, spoT*) is represented in Fig. 3. Among the analyzed genes, *rpoE* and *htrA* did not show significant differences in expression compared with SeT ($p > 0.05$). In contrast, all other genes showed significant overexpression ($p < 0.05$), ranging from approximately 0.5 to 2.5 log_2 fold change. The strongest increase in expression was observed for *rpoD*, whereas moderate increases were detected for *rpoN*, *rpoS*, *dnaK*, *soxR*, and *spoT*.

Overall, the SeT_{rpoD} mutant exhibited increased basal transcription of several stress-responsive genes prior to the inactivation treatments.

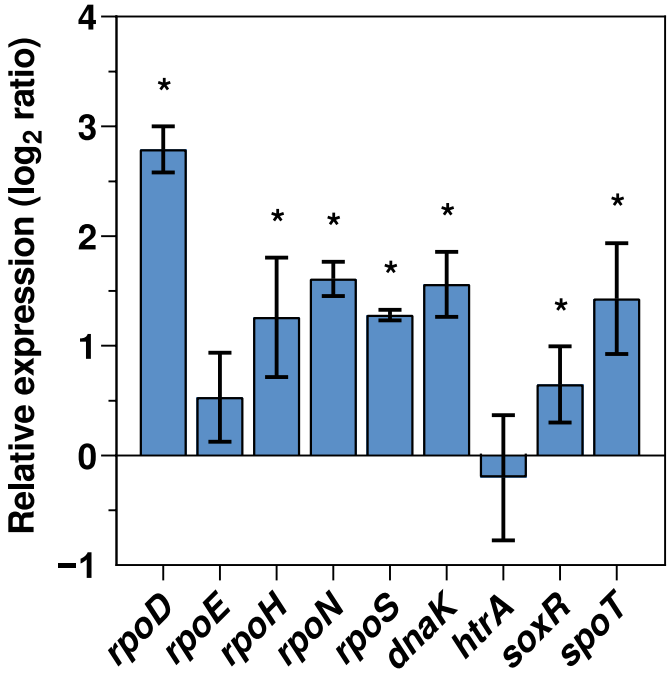

Fig. 3. Relative basal expression (log_2 ratio) of selected stress response-related genes in the *rpoD*-isogenic mutant (SeT_{rpoD}) compared with the *Salmonella enterica* subsp. *enterica* serovar Typhimurium str. LT2 parental strain (SeT). Results expressed as means ± standard deviations (error bars). Asterisks indicate significant differences after comparing normalized gene copy numbers obtained ($p \leq 0.05$).

3.4. Compensatory interactions between cross-protective mutations can preserve virulence potential

In our previous work, we assessed the virulence of SeT_{RV1} using the *Caenorhabditis elegans* nematode model (Campillo et al., 2025). To further investigate the contribution of each mutation to virulence, we evaluated the pathogenicity of SeT, SeT_{RV1}, and the corresponding isogenic mutants (SeT_{rpoD}, SeT_{cyaA}, SeT_{ramR}, $SeT_{rpoD/cyaA}$, $SeT_{rpoD/ramR}$, and $SeT_{cyaA/ramR}$) using the *Galleria mellonella* infection model, which allows incubation at 37 °C and therefore enables the assessment of temperature-dependent virulence traits (Fig. 4).

Survival curves post-injection revealed variant- and inoculum-dependent differences in virulence among SeT, SeT_{RV1} and the derived isogenic mutants. At an inoculum of 10^5 CFU/mL, SeT_{RV1} displayed slightly diminished virulence compared to SeT ($p < 0.05$). In contrast, no significant differences were observed between SeT and SeT_{RV1} at 10^4 CFU/mL. SeT_{rpoD} exhibited a consistent attenuation of virulence relative to SeT at both inoculum levels ($p < 0.05$), while the *cyaA* mutant showed no significant differences at either concentration. Interestingly, although virulence was not significantly altered at the higher inoculum, SeT_{ramR} displayed increased virulence at 10^4 CFU/mL compared to SeT ($p < 0.05$).

To determine whether the altered tolerance observed in SeT_{RV1} represents a broader consequence of CIP resistance evolution, we extended the analysis to additional RVs (SeT_{RV2}-SeT_{RV5}) carrying distinct mutations and evaluated their response to PEF and UV-C.

3.5. Cross-protection patterns across ciprofloxacin-resistant variants against PEF and UV-C

Since SeT_{RV1} did not exhibit increased tolerance to PEF, we extended the analysis to additional RVs (SeT_{RV2}-SeT_{RV5}) to explore whether other mutational backgrounds show different cross-protection patterns. In addition, the evaluation of UV-C resistance in these RVs was particularly relevant because several mutations present in SeT_{RV2}-SeT_{RV5} affect

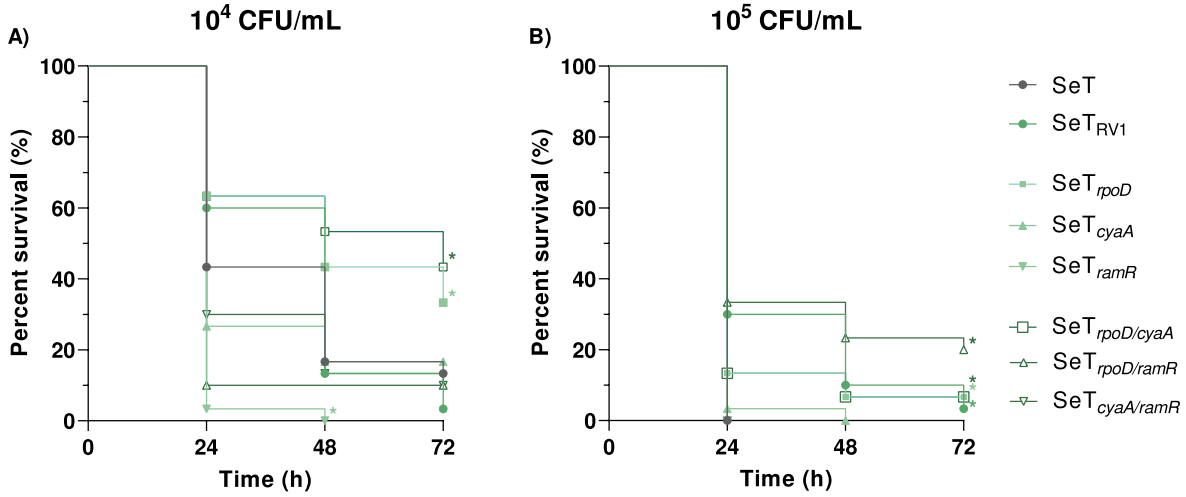

Fig. 4. Kaplan-Meier survival curves of *Galleria mellonella* larvae after being infected with *Salmonella enterica* subsp. *enterica* serovar Typhimurium str. LT2 parental strain (SeT), its ciprofloxacin-resistant variant (SeT_{RV1}) and the single- (SeT_{rpoD}, SeT_{cyaA}, SeT_{ramR}) and double-complementary strains ($SeT_{rpoD/cyaA}$, $SeT_{rpoD/ramR}$, $SeT_{cyaA/ramR}$) derived from SeT_{RV1}. Larvae were injected with bacterial suspensions at two different concentrations: **A)** 10^4 CFU/mL (continuous lines) and **B)** 10^5 CFU/mL (discontinuous lines). Survival was monitored over time, and curves represent the mean survival of three repeats of each experiment. The Mantel-Cox (log-rank) test was used to assess statistical differences in larval survival ($p < 0.05$).

DNA-related processes and oxidative stress responses, which are key targets of UV-C inactivation (Gomes et al., 2005; Narita et al., 2025). As a result, $\log_{10}$ reduction of SeT and all RVs (SeT_{RV1}-SeT_{RV5}) after PEF and UV-C treatments are presented in Fig. 5.

Again, none of the RVs exhibited significantly altered tolerance to PEF (Fig. 5A; $p > 0.05$), indicating that the alterations induced by CIP exposure in these variants did not measurably affect their susceptibility to this technology.

Interestingly, three other RVs showed significantly lower inactivation against UV-C compared to SeT (Fig. 5B; $p \leq 0.05$): 2.08 $\log_{10}$ reduction for SeT_{RV3}, 2.45 for SeT_{RV4}, and 2.71 for SeT_{RV5}. These cross-protections represent increases in survival risk ranging from *ca.* 10-fold to 100-fold after the UV-C treatments due to mutations.

4. Discussion

The current understanding of cross-protection to food preservation stresses in AMR bacteria remains limited, particularly when tolerance arises through adaptation to antibiotics rather than to food industry-related stressors, as previously introduced. Nevertheless, some precedents linked mutations conferring AMR indirectly affecting bacterial responses to heat treatments. These observations include mutations *ubi* genes associated with pleiotropic protection against heat treatments (Collis and Grigg, 1989; Søballe and Poole, 2000), and more recently, our previous work regarding acquired ciprofloxacin (CIP) resistance in *Salmonella* Typhimurium and cross-protection to thermal inactivation (Campillo et al., 2025). Building on this background, the present study extends this line of research to emerging non-thermal preservation technologies, allowing us to explore whether AMR-related mutations can also influence bacterial tolerance to physical inactivation stresses and virulence potential.

The CIP-resistant variant SeT_{RV1} displayed reduced susceptibility to UV-C and HHP treatments compared with the parental strain SeT, whereas no differences were observed for PEF (Table 2). Among the mutations present in SeT_{RV1}, the altered *rpoD* allele emerged as the primary contributor to these tolerance phenotypes (Figs. 1 and 2). As a global transcriptional regulator encoding the housekeeping sigma factor σ^{70}, RpoD directs RNA polymerase to a large proportion of bacterial

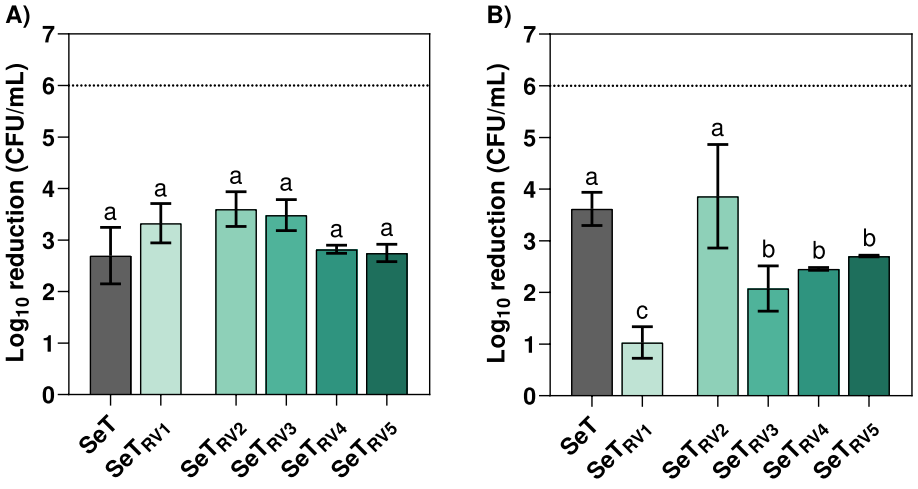

Fig. 5. Log_{10} reduction ($\log_{10}$ [N_0/N_t]) of *Salmonella enterica* subsp. *enterica* serovar Typhimurium str. LT2 parental strain (SeT) and its ciprofloxacin-resistant variants (SeT_{RV1}, SeT_{RV2}, SeT_{RV3}, SeT_{RV4}, and SeT_{RV5}) after performing lethal treatments with **A)** pulsed electric fields (30 kV/cm, 50 pulses, 1 Hz), and **B)** ultraviolet C irradiation (15 mJ/cm^2). Treatment medium was citrate-phosphate buffer at pH 7.0 for both cases. Results expressed as means ± standard deviations (error bars). N_0 ~3 × 10^7 CFU/mL. Horizontal dotted line represents the detection limit. Different letters indicate significant differences ($p \leq 0.05$).

promoters during exponential growth. Mutations affecting *rpoD* may therefore generate broad regulatory consequences by altering competition between the housekeeping sigma factor and alternative stress-responsive sigma factors (Cho et al., 2014; Gao et al., 2016; Gayán et al., 2016; Gayán et al., 2020; Park et al., 2024). The strong contribution of *rpoD* observed here, together with similar findings previously reported for thermal tolerance (Campillo et al., 2025), supports the idea that mutations affecting global transcriptional regulation may generate generalized stress-adaptation phenotypes rather than responses specific to a single environmental stressor.

The magnitude of the cross-protection observed during HHP treatments was also strongly influenced by the food matrix (Fig. 2). In particular, bacterial survival differences were considerably greater in skimmed milk than in orange juice. Such matrix-dependent differences are consistent with the known influence of food physicochemical composition on microbial inactivation. Components such as proteins, lipids, and soluble solids may exert protective effects during inactivation treatments by stabilizing cellular structures and mitigating induced damage (Zhang et al., 2022). In contrast, the acidic nature of orange juice may limit these protective effects and increase microbial inactivation due to the combined action of low pH and organic acids. However, since HHP inactivation is closely associated with membrane perturbation and protein destabilization (Sehrawat et al., 2021), the global regulatory effects associated with the *rpoD* mutation could also indirectly influence membrane-associated responses under different matrix conditions.

The phenotypic outcome of the SeT_{RV1} genotype is further shaped by interactions among the different mutations present in this variant. In particular, an antagonistic interaction between *rpoD* and *ramR* mutations was observed, which had already been reported in our previous study on thermal tolerance (Campillo et al., 2025). The RamAR regulatory system controls the expression of multiple genes involved in multidrug efflux, membrane permeability, metabolism, and virulence (Bailey et al., 2010; De Majumdar et al., 2015; Holden and Webber, 2020; Maldonado et al., 2023). Activation of RamA promotes the expression of the AcrAB-TolC efflux system and can alter membrane permeability, thereby producing widespread physiological changes affecting envelope composition and metabolic balance. Such alterations could interfere with the stress-adaptation networks activated through alternative sigma factors, thereby counteracting the protective regulatory shift associated with the *rpoD* mutation.

In contrast, *cyaA*, which encodes adenylate cyclase, regulates intracellular levels of cyclic adenosine monophosphate (cAMP), a pleiotropic second messenger controlling global transcription through the cAMP-CRP (cAMP receptor protein) regulatory system. Loss-of-function mutations in *cyaA* reduce intracellular cAMP levels and can therefore modify the expression of numerous genes involved in metabolism and stress adaptation. Reduced cAMP synthesis has previously been associated with enhanced bacterial tolerance to oxidative stress (Barth et al., 2009), which may partially explain the increased UV-C tolerance observed in strains carrying this mutation. Since UV-C irradiation induces both direct DNA damage and intracellular generation of reactive oxygen species, enhanced oxidative stress responses could contribute to improved bacterial survival following UV exposure. In addition, mutations affecting the cAMP-CRP regulatory network may alter promoter competition for RNA polymerase (Ishihama, 2000), indirectly promoting transcriptional prioritization toward stress-responsive sigma factors.

The transcriptional analyses performed provided additional support for the regulatory hypothesis underlying the observed cross-protection phenotypes (Fig. 3). In particular, the isogenic mutant SeT_{rpoD} showed basal overexpression of several stress-related genes prior to inactivation treatments. Interestingly, *rpoD* itself was the most strongly overexpressed gene. Under normal conditions, RpoD autoregulates its own transcription (Cho et al., 2014), and the increased *rpoD* expression levels observed in SeT_{rpoD} may therefore reflect disruption of this autoregulatory loop. Such attenuation of functional RpoD activity is consistent with the simultaneous overexpression of alternative sigma factors including *rpoH*, *rpoN*, and *rpoS*, whose expression is influenced by the activity of the housekeeping sigma factor (Janaszak et al., 2009). However, this interpretation is based on transcriptional data alone, and further studies addressing protein levels or promoter binding would be necessary to confirm the underlying regulatory mechanism.

Among these regulators, RpoH and RpoS play key roles in coordinating bacterial responses to environmental stress. These sigma factors activate the expression of genes involved in cellular protection, including chaperones such as *dnaK* that participate in protein folding and damage repair during stress conditions (Battesti et al., 2011; Roncarati and Scarlato, 2017). The increased expression of *dnaK* observed in SeT_{rpoD} is consistent with a generalized stress-adapted physiological state. Additionally, overexpression of *spoT* provides further mechanistic support for this interpretation. SpoT modulates intracellular levels of the alarmone (p)ppGpp, which indirectly stabilizes RpoS by limiting its proteolytic degradation (Merrikh et al., 2009). The combined upregulation of these regulatory systems may therefore generate a physiological environment favoring enhanced basal stress preparedness, potentially explaining the increased tolerance to multiple inactivation stresses observed for the *rpoD* mutant. Nevertheless, the present transcriptional analysis was restricted to the single *rpoD* mutant. Additional mutations present in SeT_{RV1} or double isogenic mutants such as $SeT_{rpoD/ramR}$ may further modulate these regulatory responses through epistatic interactions.

Virulence experiments revealed that the phenotypic consequences of these mutations extend beyond stress tolerance (Fig. 4). The *rpoD* mutation imposed a clear fitness cost, significantly reducing virulence in the *Galleria mellonella* infection model, whereas the *cyaA* mutation alone did not significantly affect pathogenicity. In contrast, the *ramR* mutation increased virulence and partially compensated for the reduction caused by *rpoD*, as observed in the $SeT_{rpoD/ramR}$ mutant. These results illustrate how compensatory interactions among mutations may shape the final phenotype of RVs. From a food safety perspective, this finding is particularly relevant since it indicates that AMR variants displaying enhanced tolerance to food preservation technologies may not necessarily exhibit reduced virulence. Compensatory mutations may therefore allow RVs to retain both increased environmental resilience and virulence potential, although the relative advantage of these traits may differ between food-processing and host-associated environments due to their distinct physiological requirements. Consequently, compensatory mutations such as *ramR* may contribute differently depending on the ecological context and selective pressures encountered.

Finally, to determine whether the tolerance patterns observed in SeT_{RV1} represent a broader outcome of CIP resistance evolution, additional RVs were also evaluated. Interestingly, no increase in tolerance was detected for PEF treatments (Fig. 5A), as described for SeT_{RV1}. This may be explained by the primary mechanism of microbial inactivation by PEF, which disrupts the cytoplasmic membrane through electroporation (Mañas and Pagán, 2005; Raso et al., 2016). As a consequence, although bacterial survival after PEF treatment may also be influenced by physiological and environmental factors, the adaptations associated with CIP resistance may have a limited impact on the membrane-associated cellular targets primarily affected by electroporation. This technological specificity highlights how the impact of AMR-associated mutations on bacterial survival may strongly depend on the cellular targets of each inactivation process.

However, several of these RVs displayed increased tolerance to UV-C (Fig. 5B). The enhanced survival observed in strains SeT_{RV3}, SeT_{RV4}, and SeT_{RV5} was associated with mutations in *gyrA* and *gyrB*, which encode the two subunits of DNA gyrase, a key enzyme involved in DNA supercoiling and fluoroquinolone resistance (Uddin et al., 2021). Mutations in these genes can modify enzyme activity and thereby alter DNA topology (Han et al., 2012). Changes in DNA supercoiling influence global transcriptional responses and have been associated with enhanced tolerance to environmental stresses (Martis et al., 2019; Prakash et al., 2009).

Oxidative stress has also been shown to induce relaxation of DNA supercoiling in *E. coli* (Weinstein-Fischer et al., 2000), which may facilitate the expression of genes involved in oxidative stress defense and DNA repair, both of which are critical for survival following UV-induced damage (Gomes et al., 2005; Narita et al., 2025).

Additional mutations affecting oxidative stress regulatory systems may further contribute to this phenotype. In particular, variants SeT_{RV3} and SeT_{RV4} harbor mutations affecting the SoxRS regulatory system, a central regulator of oxidative stress responses (Holden and Webber, 2020). Although a mutation in *soxR* is also present in the UV-C-susceptible SeT_{RV2}, its non-frameshift nature together with the presence of an additional mutation in *thrS* may reduce its functional impact. Furthermore, mutations predicted to affect *ramA* expression were detected in SeT_{RV4} and SeT_{RV5}, potentially triggering pleiotropic protective responses due to the broad physiological roles of the RamA regulator (Bailey et al., 2010; De Majumdar et al., 2015; Holden and Webber, 2020; Maldonado et al., 2023). Altogether, these findings suggest that a combination of altered DNA topology and enhanced oxidative stress responses may improve bacterial tolerance to UV-C irradiation in certain RVs.

Taken together, the results of this study demonstrate that CIP resistance can influence bacterial tolerance to certain non-thermal food preservation technologies, leading to cross-protection, cross-sensitization, or unchanged susceptibility depending on the mutational background and the mechanism of action of each technology. These findings highlight the importance of considering AMR-associated adaptive phenomena when validating emerging non-thermal preservation strategies. In practical terms, the presence of RVs displaying cross-protection may require higher treatment intensities or additional safety margins to ensure microbial inactivation, whereas consistent cross-sensitization patterns could potentially allow milder processing conditions while maintaining microbiological safety.

5. Conclusions

This study demonstrates that the acquisition of ciprofloxacin resistance in *Salmonella* Typhimurium can modify bacterial responses to selected emerging non-thermal food preservation technologies. While tolerance to PEF remained unaffected, resistance-associated mutations significantly increased tolerance to UV-C and HHP, highlighting that cross-protection is not universal but depends on both the type of stressor and the genetic background of the strain.

Mechanistically, the mutated *rpoD* allele was identified as a key contributor to the UV-C and HHP tolerant phenotype, likely through regulatory effects that enhance stress preparedness and cellular repair systems. In contrast, mutations in *gyrA* and *gyrB* in additional resistant variants were associated with increased UV-C tolerance through mechanisms potentially related to DNA topology and responses to DNA damage. The effects of these mutations on virulence were mutation-dependent, with *rpoD*-associated attenuation partially compensated by *ramR*, illustrating the complexity of genetic interactions shaping pathogen fitness.

Overall, these findings show that AMR evolution can reshape bacterial stress tolerance and virulence through multiple genetic routes. This highlights the importance of considering AMR-associated phenotypes when evaluating the efficacy of emerging food preservation technologies and assessing potential risks for food safety.

Declaration of generative AI and AI-assisted technologies in the manuscript preparation process

During the preparation of this work, the authors used ChatGPT 5.2 (OpenAI) in order to improve spelling, grammar and readability. After using this tool, the authors reviewed and critically edited the content and take full responsibility for the content of the published article.

CRediT authorship contribution statement

Raúl Campillo: Conceptualization, Investigation, Methodology, Writing – original draft, Writing – review & editing. **Ivo García-Penas:** Writing – review & editing. **Dolores Rodrigo:** Supervision, Writing – review & editing. **Daniel Berdejo:** Writing – review & editing. **Diego García-Gonzalo:** Conceptualization, Funding acquisition, Resources, Writing – original draft, Writing – review & editing. **Rafael Pagán:** Conceptualization, Funding acquisition, Resources, Supervision, Writing – original draft, Writing – review & editing.

Declaration of competing interest

None.

Acknowledgements

This research was supported by Grant PID2021-123404NB-I00 and PID2024-156601NA-I00 funded by MICIU/AEI/10.13039/501100011033, as well as by "ERDF: A way of making Europe", and the Government of Aragón (Grant Grupo AESA grant A06_23R). The Department of Science, Technology, and University Education of the Government of Aragón (Spain) provided R. Campillo and I. García-Penas with a contract to conduct their PhD theses. We also want to thank colleagues Antonio Martínez and Walter Randazzo at IATA for their kind support, and to the research group "Nuevas tecnologías de procesado de los alimentos" for providing access to their pulsed electric fields system.

Appendix A. Supplementary data

Supplementary data to this article can be found online at https://doi.org/10.1016/j.fm.2026.105177.

Data availability

Data will be made available on request.

References

Aviv, G., Gal-Mor, O., 2018. Real-time reverse transcription PCR as a tool to study virulence gene regulation in bacterial pathogens. In: Medina, C., López-Baena, F.J. (Eds.), Host-Pathogen Interactions: Methods and Protocols. Springer, New York, NY, pp. 23–32.

Bailey, A.M., Ivens, A., Kingsley, R., Cottell, J.L., Wain, J., Piddock, L.J.V., 2010. RamA, a member of the AraC/XylS family, influences both virulence and efflux in *Salmonella enterica* serovar Typhimurium. J. Bacteriol. 192 (6), 1607–1616. https://doi.org/10.1128/jb.01517-09.

Barth, E., Gora, K.V., Gebendorfer, K.M., Settele, F., Jakob, U., Winter, J., 2009. Interplay of cellular cAMP levels, σS activity and oxidative stress resistance in *Escherichia coli*. Microbiology 155 (5), 1680–1689. https://doi.org/10.1099/mic.0.026021-0.

Battesti, A., Majdalani, N., Gottesman, S., 2011. The RpoS-mediated general stress response in *Escherichia coli*. Annu. Rev. Microbiol. 65, 189–213. https://doi.org/10.1146/annurev-micro-090110-102946.

Berdejo, D., Gayán, E., Pagán, E., Merino, N., Campillo, R., Pagán, R., García-Gonzalo, D., 2022. Carvacrol selective pressure allows the occurrence of genetic resistant variants of *Listeria monocytogenes* EGD-e. Foods 11, 3282. https://doi.org/10.3390/foods11203282.

Brankatschk, R., Bodenhausen, N., Zeyer, J., Bürgmann, H., 2012. Simple absolute quantification method correcting for quantitative PCR efficiency variations for microbial community samples. Appl. Environ. Microbiol. 78 (12), 4481–4489. https://doi.org/10.1128/aem.07878-11.

Campillo, R., García-Penas, I., Merino, N., Berdejo, D., Pagán, R., & García-Gonzalo, D. (2026). Generation of custom antibiotic-resistant variants of *Salmonella* Typhimurium by genetic engineering. In M. Magnani and G. T. de Souza (Eds.), Detection and Quantification of Bacteria, Yeast, Viruses, and Protozoan in Foods and Freshwater. Springer Nature. https://doi.org/10.1007/978-1-0716-5064-6_2.

Campillo, R., García-Penas, I., López, N., Sánchez, A., Fau, A., Gómez, D., et al., 2025. Ciprofloxacin-resistant *Salmonella* typhimurium demonstrates cross-tolerance to heat treatments in liquid food matrices. Food Res. Int. 210, 116330. https://doi.org/10.1016/j.foodres.2025.116330.

Cepas, V., Soto, S.M., 2020. Relationship between virulence and resistance among Gram-negative bacteria. Antibiotics 9 (10), 719. https://doi.org/10.3390/antibiotics9100719.

Cho, B.K., Kim, D., Knight, E.M., Zengler, K., Palsson, B.O., 2014. Genome-scale reconstruction of the sigma factor network in *Escherichia coli*: topology and functional states. BMC Biol. 12 (1), 4. https://doi.org/10.1186/1741-7007-12-4.

Collis, C.M., Grigg, G.W., 1989. An *Escherichia coli* mutant resistant to phleomycin, bleomycin, and heat inactivation is defective in ubiquinone synthesis. J. Bacteriol. 171 (9), 4792–4798. https://doi.org/10.1128/jb.171.9.4792-4798.1989.

Coombs, K., Rodríguez-Quijada, C., Clevenger, J.O., Sauer-Budge, A.F., 2023. Current understanding of potential linkages between biocide tolerance and antibiotic cross-resistance. Microorganisms 11 (8), 2000. https://doi.org/10.3390/microorganisms11082000.

Dawan, J., Ahn, J., 2020. Assessment of cross-resistance potential to serial antibiotic treatments in antibiotic-resistant *Salmonella* Typhimurium. Microb. Pathog. 148, 104478. https://doi.org/10.1016/j.micpath.2020.104478.

De Majumdar, S., Yu, J., Fookes, M., McAteer, S.P., Llobet, E., Finn, S., et al., 2015. Elucidation of the RamA regulon in *Klebsiella pneumoniae* reveals a role in LPS regulation. PLoS Pathog. 11 (1), e1004627. https://doi.org/10.1371/journal.ppat.1004627.

Diez-Sánchez, E., Martínez, A., Rodrigo, D., Quiles, A., Hernando, I., 2020. Optimizing high pressure processing parameters to produce milkshakes using chokeberry pomace, 9(4), 405. https://doi.org/10.3390/foods9040405.

European Centre for Disease Prevention and Control, 2022. Assessing the Health Burden of Infections with antibiotic-resistant Bacteria in the EU/EEA, 2016-2020. ECDC, Stockholm.

European Centre for Disease Prevention and Control, 2025. Antimicrobial Resistance in the EU/EEA (EARS-Net) - Annual Epidemiological Report for 2024. ECDC, Stockholm.

Farzana, R., Jones, L.S., Rahman, M.A., Andrey, D.O., Sands, K., Portal, E., et al., 2018. Outbreak of hypervirulent multidrug-resistant *Klebsiella variicola* causing high mortality in neonates in Bangladesh. Clin. Infect. Dis. 68 (7), 1225–1227. https://doi.org/10.1093/cid/ciy778.

Gao, X., Jiang, L., Zhu, L., Xu, Q., Xu, X., Huang, H., 2016. Tailoring of global transcription sigma D factor by random mutagenesis to improve *Escherichia coli* tolerance towards low-pHs. J. Biotechnol. 224, 55–63. https://doi.org/10.1016/j.jbiotec.2016.03.012.

Gayán, E., Cambré, A., Michiels, C.W., Aertsen, A., 2016. Stress-induced evolution of heat resistance and resuscitation speed in *Escherichia coli* O157:H7 ATCC 43888. Appl. Environ. Microbiol. 82 (22), 6656–6663. https://doi.org/10.1128/AEM.02027-16.

Gayán, E., Cambré, A., Michiels, C.W., Aertsen, A., 2017. RpoS-independent evolution reveals the importance of attenuated cAMP/CRP regulation in high hydrostatic pressure resistance acquisition in *E. coli*. Sci. Rep. 7 (1), 8600. https://doi.org/10.1038/s41598-017-08958-z.

Gayán, E., Van den Bergh, B., Michiels, J., Michiels, C.W., Aertsen, A., 2020. Synthetic reconstruction of extreme high hydrostatic pressure resistance in *Escherichia coli*. Metab. Eng. 62, 287–297. https://doi.org/10.1016/j.ymben.2020.09.008.

Giacometti, F., Shirzad-Aski, H., Ferreira, S., 2021. Antimicrobials and food-related stresses as selective factors for antibiotic resistance along the farm to fork continuum. Antibiotics 10 (6), 671. https://doi.org/10.3390/antibiotics10060671.

Gomes, A.A., Silva-Júnior, A.C.T., Oliveira, E.B., Asad, L.M.B.O., Reis, N.C.S.C., Felzenszwalb, I., et al., 2005. Reactive oxygen species mediate lethality induced by far-UV in *Escherichia coli* cells. Redox Rep. 10 (2), 91–95. https://doi.org/10.1179/135100005X38833.

Guillén, S., Nadal, L., Halaihel, N., Mañas, P., Cebrián, G., 2025. Isolation and characterization of *Salmonella* Typhimurium SL1344 variants with increased resistance to different stressing agents and food processing technologies. Food Microbiol. 128, 104714. https://doi.org/10.1016/j.fm.2024.104714.

Han, J., Wang, Y., Sahin, O., Shen, Z., Guo, B., Shen, J., Zhang, Q., 2012. A fluoroquinolone resistance associated mutation in *gyrA* affects DNA supercoiling in *Campylobacter jejuni*. Front. Cell. Infect. Microbiol. https://doi.org/10.3389/fcimb.2012.00021.

Holden, E., Webber, M., 2020. MarA, RamA, and SoxS as mediators of the stress response: survival at a cost. Front. Microbiol. 11. https://doi.org/10.3389/fmicb.2020.00828.

Hong, Y., Wu, Y., Xie, Y., Ben, L., Bu, X., Pan, X., et al., 2023. Effects of antibiotic-induced resistance on the growth, survival ability and virulence of *Salmonella enterica*. Food Microbiol. 115, 104331. https://doi.org/10.1016/j.fm.2023.104331.

Ishihama, A., 2000. Functional Modulation of *Escherichia coli* RNA Polymerase, vol. 54, pp. 499–518. https://doi.org/10.1146/annurev.micro.54.1.499.

Janaszak, A., Nadratowska-Wesołowska, B., Konopa, G., Taylor, A., 2009. The P1 promoter of the *Escherichia coli rpoH* gene is utilized by σ70-RNAP or σS-RNAP depending on growth phase. FEMS (Fed. Eur. Microbiol. Soc.) Microbiol. Lett. 291 (1), 65–72. https://doi.org/10.1111/j.1574-6968.2008.01436.x.

Kay, S., Edwards, J., Brown, J., Dixon, R., 2019. *Galleria mellonella* infection model identifies both high and low lethality of *Clostridium perfringens* toxigenic strains and their response to antimicrobials. Front. Microbiol. 10. https://doi.org/10.3389/fmicb.2019.01281.

Lautan, O., Cheng, Y., Pranata, R., Chen, Y., Shi, Y.H., Chen, S., Chen, R., 2025. Antimicrobial-resistant (AMR) bacteria in the food chain: current challenges and global mitigation strategies. One Health 21, 101273. https://doi.org/10.1016/j.onehlt.2025.101273.

Li, Y., Wu, Y., Shao, J., Shi, J., Sun, L., Hong, Y., Wang, X., 2025. Stresses in the food chain and their impact on antibiotic resistance of foodborne pathogens: a review. Food Microbiol. 128, 104741. https://doi.org/10.1016/j.fm.2025.104741.

Liao, X., Ma, Y., Daliri, E.B.M., Koseki, S., Wei, S., Liu, D., et al., 2020. Interplay of antibiotic resistance and food-associated stress tolerance in foodborne pathogens. Trends Food Sci. Technol. 95, 97–106. https://doi.org/10.1016/j.tifs.2019.11.006.

Livak, K.J., Schmittgen, T.D., 2001. Analysis of relative gene expression data using real-time quantitative PCR and the $2^{-\Delta\Delta CT}$ method. Methods 25 (4), 402–408. https://doi.org/10.1006/meth.2001.1262.

Álvarez-Molina, A., de Toro, M., Ruiz, L., López, M., Prieto, M., Alvarez-Ordóñez, A., 2020. Selection for antimicrobial resistance in foodborne pathogens through exposure to UV light and nonthermal atmospheric plasma decontamination techniques. Appl. Environ. Microbiol. 86 (9). https://doi.org/10.1128/AEM.00102-20 e00102-00120.

Mañas, P., Pagán, R., 2005. Microbial inactivation by new technologies of food preservation. J. Appl. Microbiol. 98 (6), 1387–1399. https://doi.org/10.1111/j.1365-2672.2005.02561.x.

Maldonado, J., Czarnecka, B., Harmon, D.E., Ruiz, C., 2023. The multidrug efflux pump regulator AcrR directly represses motility in *Escherichia coli*. mSphere 8 (5). https://doi.org/10.1128/msphere.00430-23 e00430-00423.

Martis, S., Forquet, R., Reverchon, S., Nasser, W., Meyer, S., 2019. DNA supercoiling: an ancestral regulator of gene expression in pathogenic bacteria? Comput. Struct. Biotechnol. J. 17, 1047–1055. https://doi.org/10.1016/j.csbj.2019.07.013.

Merrikh, H., Ferrazzoli, A.E., Lovett, S.T., 2009. Growth phase and (p)ppGpp control of irad, a regulator of RpoS stability. Escherichia coli 191 (24), 7436–7446. https://doi.org/10.1128/jb.00412-09.

Milani, E.S., Hasani, A., Varschochi, M., Sadeghi, J., Memar, M.Y., Hasani, A., 2021. Biocide resistance in *Acinetobacter baumannii*: appraising the mechanisms. J. Hosp. Infect. 117, 135–146. https://doi.org/10.1016/j.jhin.2021.09.010.

Ménard, G., Rouillon, A., Cattoir, V., Donnio, P.-Y., 2021. *Galleria mellonella* as a suitable model of bacterial infection: past, present and future. Front. Cell. Infect. Microbiol. 11. https://doi.org/10.3389/fcimb.2021.782733.

Narita, K., Fukushi, R., Yamane, K., Okumura, Y., Koi, T., Asano, K., Nakane, A., 2025. Reactive oxygen species generated by irradiation with bandpass-filtered 222-nm Far-UVC play an important role in the germicidal mechanism to *Escherichia coli*, 91(2), e01886-01824. https://doi.org/10.1128/aem.01886-24.

Oniciuc, E.A., Likotrafiti, E., Álvarez-Molina, A., Prieto, M., López, M., Álvarez-Ordóñez, A., 2019. Food processing as a risk factor for antimicrobial resistance spread along the food chain. Curr. Opin. Food Sci. 30, 21–26. https://doi.org/10.1016/j.cofs.2018.09.002.

Pagán, E., Merino, N., Berdejo, D., Campillo, R., Gayán, E., García-Gonzalo, D., Pagán, R., 2024. Adaptive evolution of *Salmonella* Typhimurium LT2 exposed to carvacrol lacks a uniform pattern. Appl. Microbiol. Biotechnol. 108 (1), 38. https://doi.org/10.1007/s00253-023-12840-6.

Park, E., Ha, J., Oh, H., Kim, S., Choi, Y., Lee, Y., et al., 2021. High prevalence of *Listeria monocytogenes* in smoked duck: antibiotic and heat resistance, virulence, and genetics of the isolates. Food Science of Animal Resources 41 (2), 324–334. https://doi.org/10.5851/kosfa.2021.e2.

Park, J.Y., Jang, M., Lee, S.-M., Woo, J., Lee, E.J., Kim, D., 2024. Unveiling the novel regulatory roles of RpoD-family sigma factors in *Salmonella* Typhimurium heat shock response through systems biology approaches. PLoS Genet. 20 (10), e1011464. https://doi.org/10.1371/journal.pgen.1011464.

Prakash, J.S.S., Sinetova, M., Zorina, A., Kupriyanova, E., Suzuki, I., Murata, N., Los, D. A., 2009. DNA supercoiling regulates the stress-inducible expression of genes in the cyanobacterium *Synechocystis*. Mol. BioSyst. 5 (12), 1904–1912. https://doi.org/10.1039/B903022K.

Raso, J., Frey, W., Ferrari, G., Pataro, G., Knorr, D., Teissie, J., Miklavčič, D., 2016. Recommendations guidelines on the key information to be reported in studies of application of PEF technology in food and biotechnological processes. Innov. Food Sci. Emerg. Technol. 37, 312–321. https://doi.org/10.1016/j.ifset.2016.08.003.

Roncarati, D., Scarlato, V., 2017. Regulation of heat-shock genes in bacteria: from signal sensing to gene expression output. FEMS (Fed. Eur. Microbiol. Soc.) Microbiol. Rev. 41 (4), 549–574. https://doi.org/10.1093/femsre/fux015.

Samtiya, M., Matthews, K., Dhewa, T., Puniya, A., 2022. Antimicrobial resistance in the food chain: trends, mechanisms, pathways, and possible regulation strategies. Foods 11 (19). https://doi.org/10.3390/foods11192966.

Søballe, B., Poole, R.K., 2000. Ubiquinone limits oxidative stress in *Escherichia coli*. Microbiology 146 (4), 787–796. https://doi.org/10.1099/00221287-146-4-787.

Sehrawat, R., Kaur, B.P., Nema, P.K., Tewari, S., Kumar, L., 2021. Microbial inactivation by high pressure processing: principle, mechanism and factors responsible. Food Sci. Biotechnol. 30 (1), 19–35. https://doi.org/10.1007/s10068-020-00831-6.

Song, K., Mohseni, M., Taghipour, F., 2019. Mechanisms investigation on bacterial inactivation through combinations of UV wavelengths. Water Res. 163, 114875. https://doi.org/10.1016/j.watres.2019.114875.

Tsai, C.J., Loh, J.M., Proft, T., 2016. *Galleria mellonella* infection models for the study of bacterial diseases and for antimicrobial drug testing. Virulence 7 (3), 214–229. https://doi.org/10.1080/21505594.2015.1135289.

Uddin, M.K.M., Ather, M.F., Nasrin, R., Rahman, T., Islam, A., Rahman, S.M.M., Ahmed, S., 2021. Correlation of *gyr* mutations with the minimum inhibitory concentrations of fluoroquinolones among multidrug-resistant *Mycobacterium tuberculosis* isolates in Bangladesh. Pathogens 10 (11). https://doi.org/10.3390/pathogens10111422.

Walsh, C., Duffy, G., Sheridan, J.J., Fanning, S., Blair, I.S., McDowell, D.A., 2005. Thermal resistance of antibiotic-resistant and antibiotic sensitive *Salmonella* spp. on chicken meat. J. Food Saf. 25 (4), 288–302. https://doi.org/10.1111/j.1745-4565.2005.00021.x.

Walsh, D., Sheridan, J.J., Duffy, G., Blair, I.S., McDowell, D.A., Harrington, D., 2001. Thermal resistance of wild-type and antibiotic-resistant *Listeria monocytogenes* in meat and potato substrates. J. Appl. Microbiol. 90 (4), 555–560.

Weinstein-Fischer, D., Elgrably-Weiss, M., Altuvia, S., 2000. *Escherichia coli* response to hydrogen peroxide: a role for DNA supercoiling, Topoisomerase I and Fis. Mol. Microbiol. 35 (6), 1413–1420.

Yang, Q., Li, M., Spiller, O.B., Andrey, D.O., Hinchliffe, P., Li, H., et al., 2017. Balancing MCR-1 expression and bacterial survival is a delicate equilibrium between essential cellular defence mechanisms. Nat. Commun. 8 (1), 2054. https://doi.org/10.1038/s41467-017-02149-0.

Yun, J.J., Heisler, L.E., Hwang, I.I.L., Wilkins, O., Lau, S.K., Hyrcza, M., et al., 2006. Genomic DNA functions as a universal external standard in quantitative real-time PCR. Nucleic Acids Res. 34 (12). https://doi.org/10.1093/nar/gkl400 e85.

Zhang, Y., Pérez-Reyes, M.E., Qin, W., Hu, B., Wu, Q., Liu, S., 2022. Modeling the effect of protein and fat on the thermal resistance of *Salmonella enterica* Enteritidis PT 30 in egg powders. Food Res. Int. 155, 111098. https://doi.org/10.1016/j.foodres.2022.111098.